Investigation of generative design for powder bed fusion technology in case of Formula Student race car components using Ti6Al4V alloy

Tamás Markovits [a],[*], Bence Szederkényi [b]

[a] *Department of Automotive Technologies, Faculty of Transportation Engineering and Vehicle Engineering, Budapest University of Technology and Economics, Műegyetem rkp. 3., H-1111 Budapest, Hungary*
[b] *Department of Polymer Engineering, Faculty of Mechanical Engineering, Budapest University of Technology and Economics, Műegyetem rkp. 3., H-1111 Budapest, Hungary*

ARTICLE INFO

ABSTRACT

In case of the racing car of the Formula Student competition, there was a need to use more modern solutions in the development of metallic parts. In the context of the joint research on the applicability of metal additive manufacturing, a methodology has been developed that will enable more efficient use of metallic parts in the future, from component selection across the generative design and 3D printing process steps to the validation of the results. As a further result of the research, we applied the new methodology to the 4 rocker components in the suspension of the racing car chassis, and as a result, we achieved a weight reduction of 40 % per component and three times higher load capacity. The built-in rocker's in-service testing and final approval took place on the ZalaZone proving ground.

1. Introduction

In the development of automotive components, processes and methods that provide a unique, targeted solution to a specific challenge are becoming more widespread. These processes also include generative design and 3D printing technology [1]. Combining the two methods allows new component solutions that did not exist before [2].

Generative design is a powerful tool to realize product optimization in AM [3]. One of the reasons for using topology optimization and generative design is the creation of new constructions that can be designed with less material and less weight [4,5]. The need for weight reduction [6] in vehicles is self-evident [7]. It is also important in the aircraft industry [8,9,10], but it may also be needed in the building industry [11,12] in medical application [13] and many other areas [14].

The analysis and methodological development [15] of the advantages and disadvantages [16,17] of design methods related to additive production is currently underway to achieve better constructions. Along with the increasing discovery of challenges and barriers [18], an analysis and comparison of the software used to apply generative design also show that it is important to consider the differences in their selection [19].

Due to the rapid development, metal 3D printing technology has also appeared in component manufacturing. Applying additive

manufacturing, previous component designs can be replaced with new design solutions, which is also greatly aided by generative design [20]. One of the main application areas is the production of customized components, where complex component geometries with a smaller number of pieces can be made with a shorter lead time [21].

Additive manufacturing (AM) such as laser powder bed fusion (LPBF) or selective laser melting (SLM) enable enormous freedom for the design of the complex structure, deviations between as-designed and as-manufactured shape [22]. New designs emerge that provide new solutions compared to traditional manufacturing technologies through the creation and manufacturability of topology optimization, generative design, and unique structured structures or surfaces (lattice design) [23]. The use of lattice structures is an area that is becoming more and more feasible [24] in the case of metals and polymers [25] and different constructions with different strategies [26].

Comparing the printing of metals and polymers, the technology for metals is more complex and less well known. Its exploration and research are still ongoing, and more and more knowledge is available.

Print preparation is one of the most important steps to successful printing, the effect of supports and parameters on printability [27] and model properties is also determined [28]. In the case of metallic additive manufacturing, the support of parts and models is an essential task due to mechanical fixation and heat removal. However, the use of material,

subsequent removability and deterioration of surface properties at the site of supports may be detrimental [29]. It is a strong effort to reduce or even eliminate the amount of support. In case it cannot be left out due to easier removal, the development of contact-free support is also under research [30]. Another development direction is to develop other types of support solutions [2] that can provide additional benefits during manufacturing or post-processing [31].

The printed model's material structure, geometry, and surface properties have become increasingly explored [32]. Fatigue properties are also intensively researched under dynamic loads [33], supplemented, where appropriate, by examining the effect of the stress-relieving heat treatment [34]. Performing fatigue tests is a resource and time-consuming process, and this is not always appropriate for components designed for short life, such as competitive sports and for the parts used there. There is a need for a different solution.

The spread of advanced solutions within the automotive industry in competitive sports started a few years ago [35]. The Formula Racing Team (FRT) at the BME university is also taking advantage of the additive manufacturing components, as has already begun for foreign teams.

Generative design and metal additive manufacturing is increasingly used in the Formula Student international competition series [36]. Within this, they also deal with the selection of steel, aluminium [37,38] and titanium components, as well as chassis, suspension components [21] and brake system components [39], crank components [35], roll steering elements [40]. In the case of the aluminium racing car part, a comparison of the part made with the milled and the generative design showed a larger area of freedom [41]. There are also several application examples in the case of vehicles where seatbelt bracket [42], frame structure [43]. Some research results are presented in the literature, but the whole process is not shown. Therefore, it was necessary to develop this whole methodology.

The significance of the use of additive manufacturing in this case is that as a result of a faster component development process, components
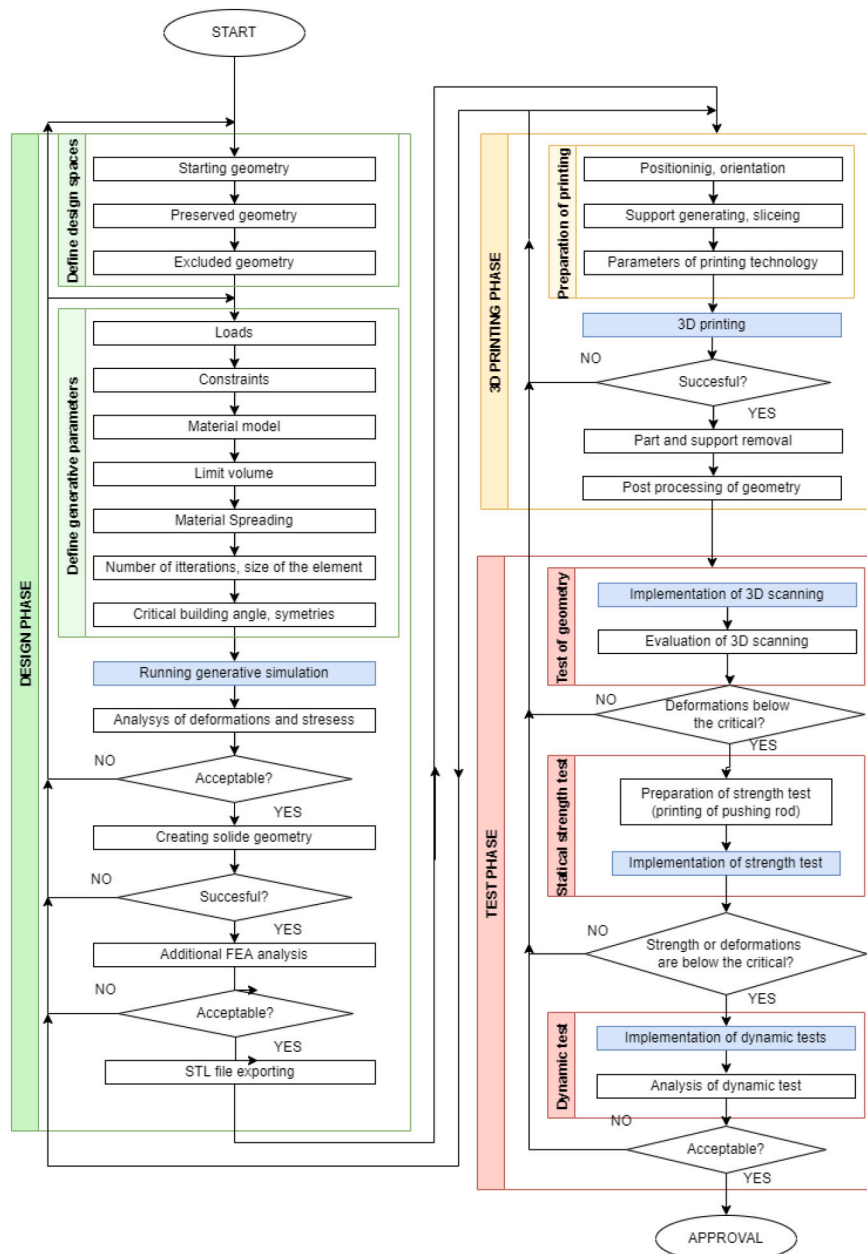

Fig. 1. Process flow of the developed methodology.

with lower weights can be produced with complex geometries that are difficult to achieve with conventional manufacturing.

The research aimed was to develop a methodology for more efficient development of new components, from selection of components through the application of generative design, using metal powdered 3D printing, to testing and validating the printed models. An additional goal was to use the new methodology to develop a unique component that provides an additional competitive advantage over a specific component, with fewer parts, lower weight and higher load bearing capacity.

2. Experiments

In the course of the research, a research methodology has been developed. It consists of three main phases: the design phase, the 3D printing phase and the test phase. Each phase consists of a series of separate steps. We present a flowchart in Fig. 1 to visualise this methodology with the main steps.

The design principles were that the new components would perform the same function, with less weight, where excess material would be removed, and the design should be such that the number of components used could be reduced, thus reducing the number of assembly times and the possibility of failures.

As the first step in research work, we analysed the existing components in the racing car. After analysing the components of the FRT team's racing car and taking into account other boundary conditions (material, functions, weight of the existing components, size of the building chamber of the 3D printer), four chassis rockers were finally selected. These parts were initially made of aluminium AA7075 with laser cutting and finally assembled from nine different elements. The position of the rocker parts on the race car and the main elements of the original aluminium construction can be seen in Fig. 2.

2.1. Generative design of rockers

The new construction design was realized by applying the generative design process in Creo 7.0.2 software to develop the original rocker part. The main steps of generative design were: defining the design spaces (geometries), specifying the generative parameters, running the generative design process, and post-processing (more precise FEA (finite element analysis) and file conversion). An STL file was created as output.

Two versions (A and B) were examined when determining the different design spaces. In the first version, we used excluded geometry and preserved geometry only in the immediate vicinity of the four connecting points, and we also designed the contact surfaces by longer cylinders. In the case of version B, the spaces due to the movement possibility of suspension components were also considered in the case of excluded geometry, so the volume that the software can design was more limited. The two versions of the design space are shown in Fig. 3.

To define the loads and constraints due to the function, we used cylindrical surfaces through which the rocker part is connected to the other elements of the suspension. The part was fixed in the hole with the largest diameter, and different axial and radial forces were defined in the other cylindrical surfaces. Finally, we defined 12 different forces, and their values were varied in different setups. The location and direction of the different forces defined during generative design are shown in Fig. 4.

By setting these forces to different values, different geometries were obtained. The best six generative setups are finally shown in Table 1. with the values of the applied forces.

During generative design, different limit volumes, material spreading, fidelity, minimum element size, and a number of iterations were applied. Each value is shown in Table 2. for six different generative setups. In the case of limit volume, we also tried to give percentages and weights, giving different results.

The material model used in the generative design was the Ti6Al4V alloy, and the properties were determined by our measurement on the printed specimens earlier, such as tensile strength, yield strength and Young's modulus. Thus, the material properties were given based on our printed parts.

In connection with the generative software used, our experience was that the stress and strain results obtained during the generative process were rough values, so the subsequent finite element analysis of the selected part was performed separately before printing. The required deformation and stress analysis was also performed in Ansys 2020R2 software with the selected geometry (in the case of generative setup 6). The main parameters of the analysis can be seen in Fig. 5.

2.2. Printing the models

The applied powder material was the commercially available EOS Ti6Al4V (EOS Titanium Ti64 9011-0039). The composition of the material can be seen in Table 3. The particle size distribution can be characterised by the $d50 = 39 \pm 3$ µm according to ISO 13320.

An EOS M100 laser-based powder bed fusion machine was used for the printing. The unit has a cylindrical working space of ø 100×95 mm, and a disc shape building platform was used with a thickness of 15 mm. The applied fiber laser has a maximal power of 200 W. The default EOS technology parameters were used for 20 micrometre building layer thickness, consisting of one hundred parameters. For titan material, the Ti64_020_FlexM100_100 default parameter set was applied.

A critical part of preparing for printing is determining the orientations during which the printing time and the amount of support material can vary greatly. With certain orientations, the process may stop with an error during printing. Table 4 presents some of these orientations that have been considered in the research as possible solutions. We show the amount of support required for these orientations and the evolution of printing times.
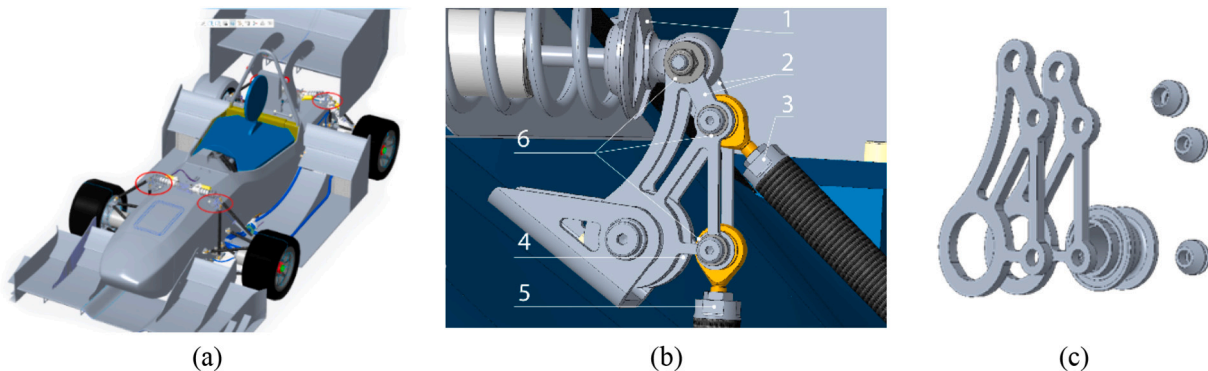

(a) (b) (c)

Fig. 2. The selected car parts (a) racing car, (b) the rocker built-in, (1: damper, 2: rocker frame, 3: push rod, 4: bearing house, 5: pull rod, 6: washers), (c) nine elements of original rocker.
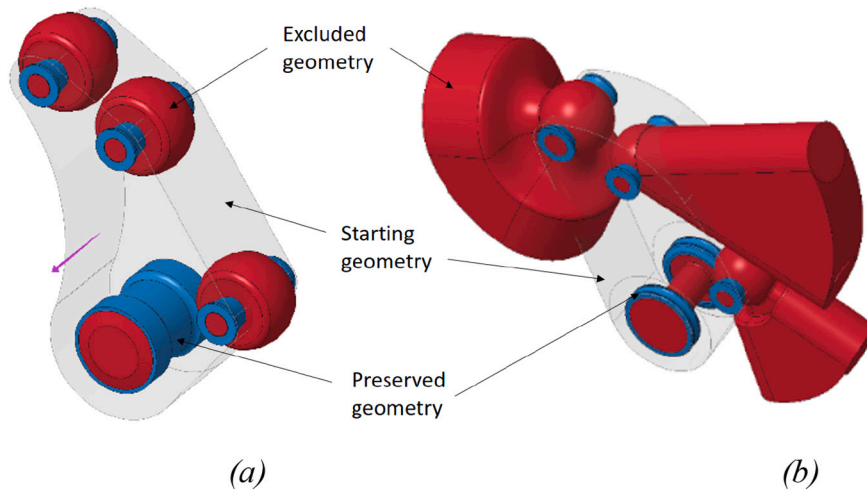
Fig. 3. The applied design spaces in the generative module (a) version A, (b) version B.
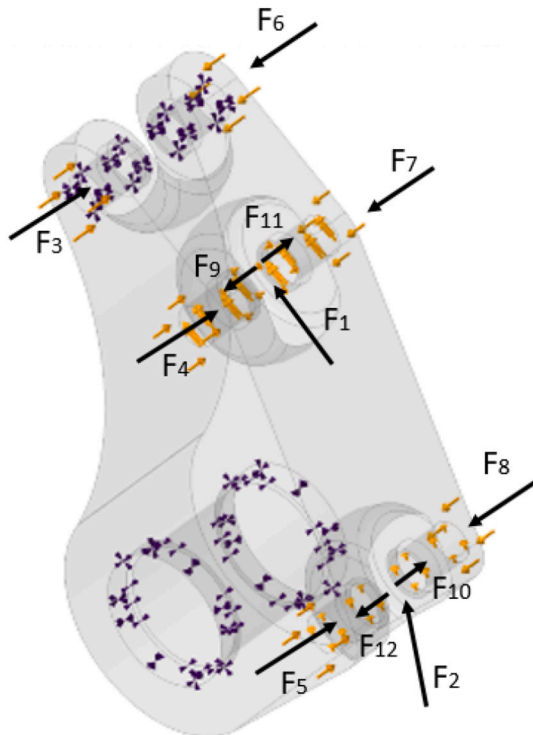

Fig. 4. Illustration of the applied mechanical loads and the constraints.

Examination of the different model orientations has shown that the shortest printing time is achieved with the C-type orientation, even if it does not provide the least support material requirements. Since the production time for this technology is the one that determines the costs the most, we have chosen the orientation that provides the shortest

printing time. Higher building orientations would have required more slender support, which is dangerous for the technology to vibrate, so the use of A and B orientations was discarded for this reason as well.

The supported model can be seen in the printed orientation on the building platform in Fig. 6. Due to the easier detachability of the model, we used a teeth between the support and the model that can perform the mechanical fixation and allows easy detachment.

After the ten-hour printing operation, the part is shown in Fig. 7 when it is removed from the equipment workspace but not yet disconnected from the building platform.

Measuring stress levels after printing is difficult, especially in complex geometry. The print stress is estimated using simulation software, where the calibration in the software is performed using so-called cantilever components. The orientation and support types defined during print preparation can be read into the simulation software, and the specific technology used can be taken into account during calibration.

To evaluate the print stresses, we performed print simulations using Simufact Additive software, suitable for estimating the stresses and their distribution during the different operation steps. The first operation step is the status after printing when the part is still attached to the platform and the support. The second step is the internal support was removed from the different surfaces of the model, and it severed the physical connection between several rods. This status shows the stress status at the time of later usage. The stress values simulated at each point in the different states are presented in the results section. The points selected for comparison are shown in Fig. 8.

2.3. Validation of printed parts

After the printing, the parts were analysed from the viewpoints of the geometry, the static strength and the dynamic loads. These experimental processes are detailed in the next chapter.

2.3.1. Validation of geometry
Printed parts were tested from the viewpoint of geometrical fitting

Table 1
The values of the applied forces in case of different generative setups.

Number of generative setup	F1 (N)	F2 (N)	F3 (N)	F4 (N)	F5 (N)	F6 (N)	F7 (N)	F8 (N)	F9 (N)	F10 (N)	F11 (N)	F12 (N)
1	4500	450	12,500	9000	9000	12,500	9000	9000	850	0	850	0
2	4500	450	12,500	9000	9000	12,500	9000	9000	850	0	850	0
3	4500	450	12,500	9000	9000	12,500	9000	9000	850	0	850	0
4	4500	450	0	0	0	0	0	0	1000	100	0	0
5	4500	450	0	0	0	0	0	0	1000	100	0	0
6	4500	450	0	0	0	0	0	0	1000	100	0	0

Table 2
The applied generative parameters in case of different setups.

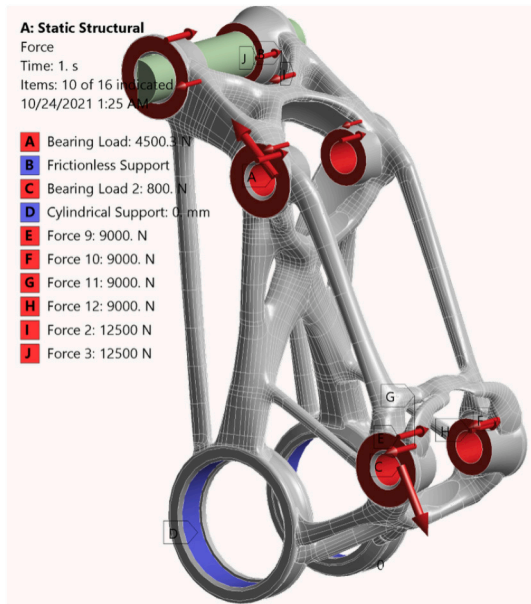| Number of generative setup	Version of design space (A or B)	Limit volume (%)	Limit volume (g)	Material spreading (%)	Fidelity (–)	Minimum element size (mm)	Maximum number of iteration (–)
1	A	35	–	100	5	0,943	330
2	A	30	–	–	5	0,943	330
3	A	15	–	80	7	0,743	472
4	B	–	60	100	7	0,743	472
5	B	–	50	–	6	0,907	399
6	B	–	48	–	6	0,907	399

Fig. 5. The main parameters of finite element analysis.

because the printed metals part can deform during printing due to internal stresses, especially in the case of titanium alloy. It can happen in a state when the model is fixed to the platform, but most importantly when the part is removed from the building platform or the supports are removed from the model. Thus the internal stresses can deform the part more freely. This is a phenomenon that can be reduced by stress relief heat treatment, and as a result, harmful deformations can be reduced.

Due to the complex geometry, traditional geometry measurement methods cannot be used here, such as coordinate measurement techniques, but different 3D scanners and procedures can be used. In our case, we used a laser beam measurement procedure performed on a ScanTech measuring head with a resolution of 0.05 mm. The part was scanned from different directions during the measurement, and the obtained point clouds were fitted in Geomagic Design X software as an STL file. By matching the output CAD file with the original CAD file, an Ansys SpaceClaim software was used, and we can obtain the geometric differences at different points on the part.

2.3.2. Validation of strength by static tests

In our case, the most important factor was the deformation of the printed part under to the maximal load. There are several measurement methods for determining deformations. Conventional methods include

strain gauges, inductive transducers, or full-body photo elastic examinations. These usually require a lot of preparation and expensive tools and instruments. Today, however, digital image correlation (DIC) methods analyse the specimen by processing photographs of the specimen using the analysis of pixel distances between reference points found in the images. The DIC is a remote sensing procedure that detects the entire displacement and elongation fields on visible parts of the specimen. The great advantage of this method is that it is not necessary to know the location of the failure in advance, as the measurement procedure can cover the entire specimen, and the results can be processed afterwards. The preparation of the measurement involved, on the one hand, "marking" the specimen, painting it black with acrylic paint and then finally spraying dots with white paint onto the specimen surface, and, on the other hand, setting up and calibrating the DIC cameras and strength test machine. The marking was necessary with the help of the DIC camera, as the raw surface of titanium had not contrast high enough for the equipment. The test lasted until the failure of the specimen. We were also able to extract the failure data, determining the static safety factor of the part. The tests were carried out with a Zwick Z250 machine. The special pushing head was designed, and 3D printed to make the setup as realistic as possible. A 250 kN measuring cell was applied, and the speed of the head was set to 2 mm/min. The DIC was used with a 10 Hz sampling rate. The static test setup can be seen in Fig. 9.
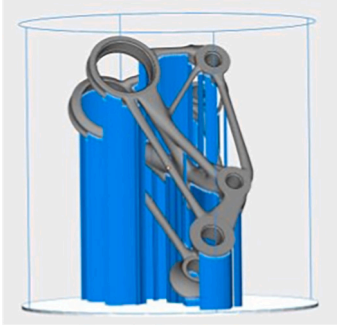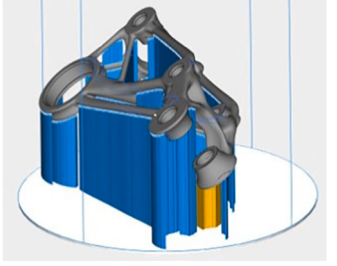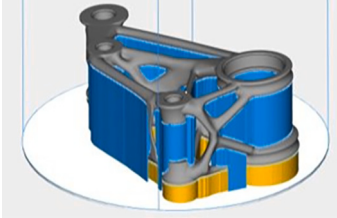
2.3.3. Dynamic validation under operating conditions

In the case of dynamic tests, due to the service life of the parts is just for one season (some months), a fatigue test was not performed. Thus the parts immediately went into the operational test phase. However, applying the operating conditions, the validation was performed on ZalaZone proving ground, where everything was available to carry out the dynamic tests.

The tests required a test track where the tests could be carried out safely in a closed area with the measurement infrastructure, even in the case of unexpected events. Our team was given the opportunity by the proving ground in Zalaegerszeg, Hungary, for a week to do critical test kilometres with the newly built car at the beginning of the season. We designed this set of test for simulating the main test of the races planned for the season, where we tested all the essential parameters of the car. A test track line was planned and carried out from the track lines occurring during the racing season with different paths, speeds and accelerations. The movements of the suspension system were recorded, and the acting forces were calculated subsequently. We also conducted several tests with the car on the track, which gave a representative test result after five days of the car's abilities. We have collected nearly 150 km in this interval, which is a large part of the total 680 km covered by our season. The proving ground and the test track can be seen in Fig. 10.

The car has several data recording sensors from which we can

Table 3
The composition of the applied Ti6Al4V powder material.

Elements	Al	V	O	N	C	H	Fe	Y	Other each	Other total	Ti
Min (wt%)	5.5	3.5									
Max (wt%)	6.75	4.5	0.2	0.05	0.08	0.015	0.3	0.005	0.1	0.4	Balance

Table 4
The prediction of the needed support material and the printing time depending on the model orientations.

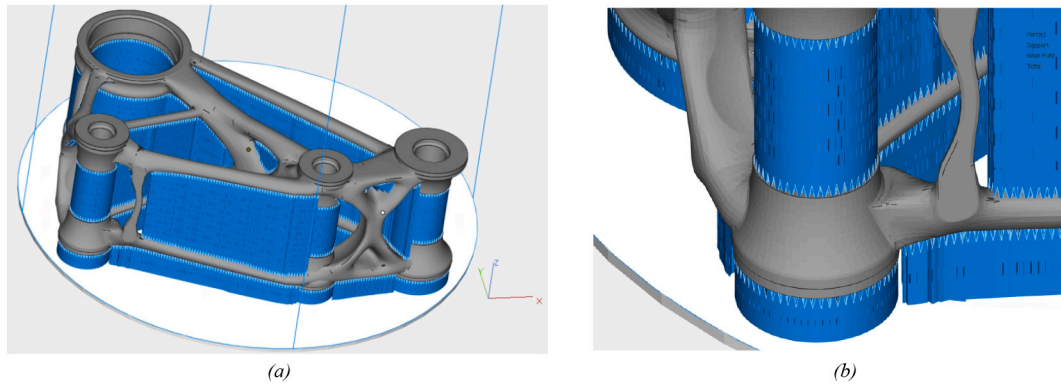| Investigated orientations	Picture of the model in the workplace	Weight of the support (g)	Printing time (h)
Orientation A		55	17,5
Orientation B		89	13,2
Orientation C		67	10,1

Fig. 6. Illustration of the prepared printing model (a) orientation and supporting of the model, (b) teeth connection between the model and the support.

determine complex vehicle dynamics data directly or indirectly. In our case, we could conclude the loads on the suspension system from the lateral acceleration values. In addition, the displacement of the suspension is recorded by a push rod sensor on each of the four wheels separately. Since these data were available to us on tracks with the same characteristics as the previous suspension. We were able to compare them with the values of the new suspension.

3. Results

The results are presented according to a similar theme as the experiments. Accordingly, we will be able to see the results for generative design, printing, and the different validation steps.

3.1. Result of generative design

Going through the generative design steps presented in the methodology, we obtained different generative designs for the different generative setups. In the case of design spaces version A, which can be seen in Fig. 11, it can be observed that the larger cylinder geometry was applied. There are also large differences in the distribution of the material in the model. Several designs have been made where only the smaller holes have been connected, so the load distribution is not even.

The resulting designs in version B are shown in Fig. 12. In these cases, the cylinders have already been connected more realistic and completely, and the load distribution was more even in the part. We can see the effect of the material spreading and limit volume parameters on
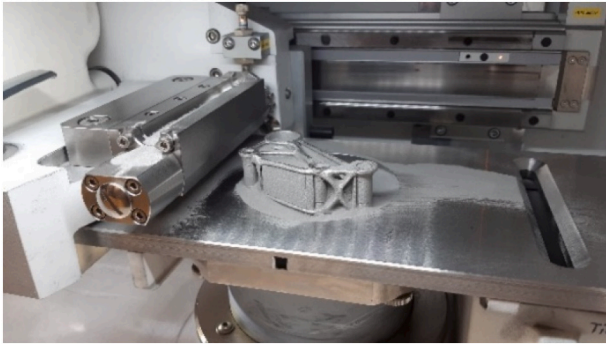
Fig. 7. The workspace of the EOS M100 equipment after the printing is finished.
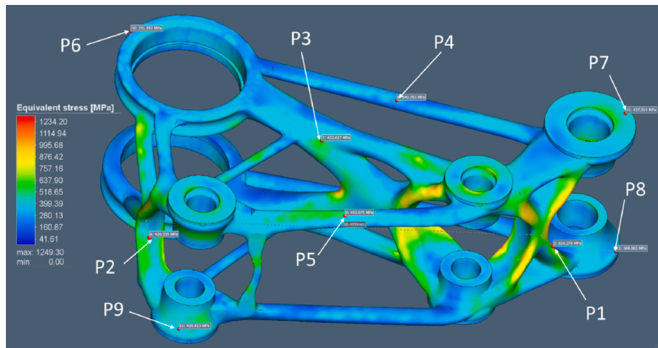

Fig. 8. Placement of points to compare simulated print stress results.
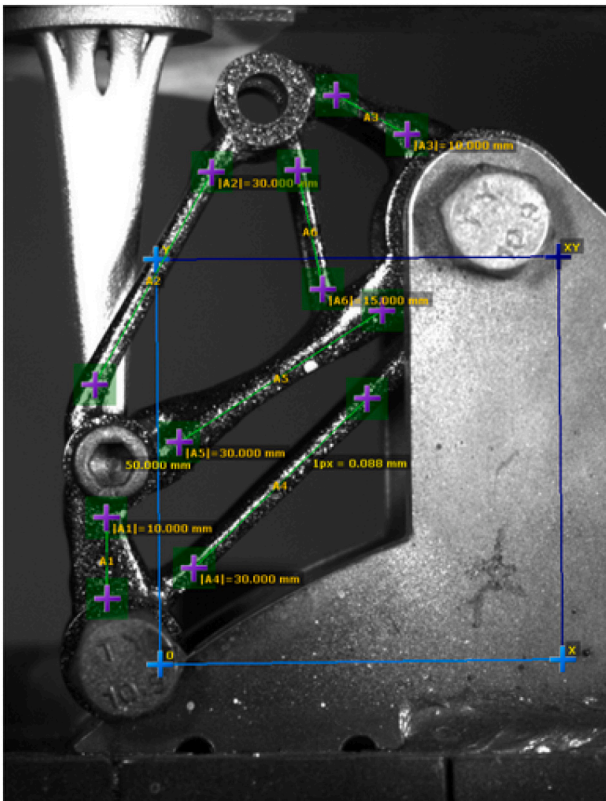

Fig. 9. The static measuring test setup with DIC system.

the generated design. Evaluating the obtained constructions shows how substantial the effect of specifying the design space is, and in the case of different acting forces and different generative parameters, significantly different geometries are obtained for the same function. Overall, setup six were selected and printed from the resulting designs because of the lowest mass.

In the finite element analysis, the stresses and strains that the part is subjected to during operation are determined, and the output shown in Fig. 13 is shown accordingly. It was concluded that the part fully met the previously established deformation and failure criteria. While only 76 % of the maximum deformation is occurred in the part under maximum loads, the yield strength of the Ti6Al4V alloy peaked at around 228 MPa, based on the simulation. This gives a safety factor of 5 for static stress.

3.2. Result of printing

Due to the satisfactory print orientation and well-selected support design in print preparation steps, the part was successfully printed after 10 h. The model connected to the building platform removed from the printer equipment is shown in Fig. 14 with and without internal support. The removal of the internal support was done by manual means due to the complex geometry of the part, so conventional cutting or other methods could not be applied. Examining the model revealed that in some places, the internal stresses caused such deformation during printing that the support and the model were partially separated in some places.

The resulting printed model is shown in Fig. 14, where all support has been removed after disconnection from the building platform. The collected support and the completed model can be observed in Fig. 15. After printing, the surfaces were shot blasted and followed by validation measurements.

Analysing the amount of powder used in the printing, we determined the model's weight and support and the total weight. The diagram showing the data is shown in Fig. 16. It can be seen that the weight of the support is significant compared to the total weight, which is because the part had to be supported in several places due to the printing orientation. By choosing a different print orientation, it would have been possible to reduce the amount of support, but this would have increased the printing time, which would have been disadvantageous for us in this case.

During printing, the powder entering the printer workspace is used in 3 different ways. The first is the amount of powder from which the model is created, the second is from which the support is built, and the third is with which it enters the exhaust system during printing for several hours. The amount of powder entering the exhaust system can also be compared to the model's proportions or the support. Therefore, this should be taken into account when planning powder usage. The results of the weight measurements show that there was a slight difference compared to the previously estimated weights.

Investigating the microstructure of the model, a typical micrograph can be seen in Fig. 17. As other researchers presented [44], Ti6Al4V material consists of columnar prior-β grains filled with acicular α' martensite, which causes high yield strength but limited ductility in case of powder bed fusion. This microstructure can be seen in our case too.

The results obtained during the print simulation used to predict the print stresses are shown in Fig. 18. The diagram shows the simulated stress values of the nine selected points (P1-P9) for different operation steps. The nine selected points are located at different places in the model, thereby representing the entire part. In the simulated stress values, it can be seen that within the elastic range, values below the yield point of the material are formed in the post-print state, which shows a relatively high value compared to our expectations.

After support removal the stress values typically decreased. The rate of stress reduction can be as high as 60 %. Only one case shows a slight increase compared to the after cutting condition. In general, the higher stress state at the end of printing decreases with the loss of fixation,
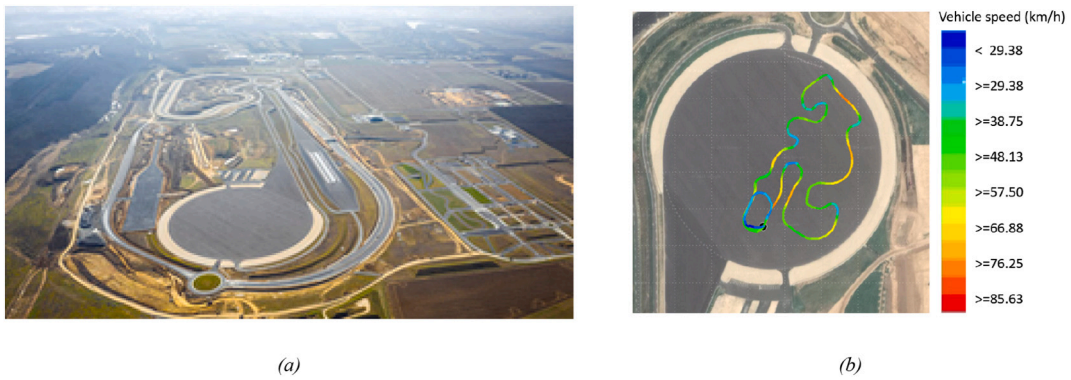
Fig. 10. Place of the dynamic tests (a) ZalaZone proving ground, (b) test track and vehicle speeds on dynamic platform.
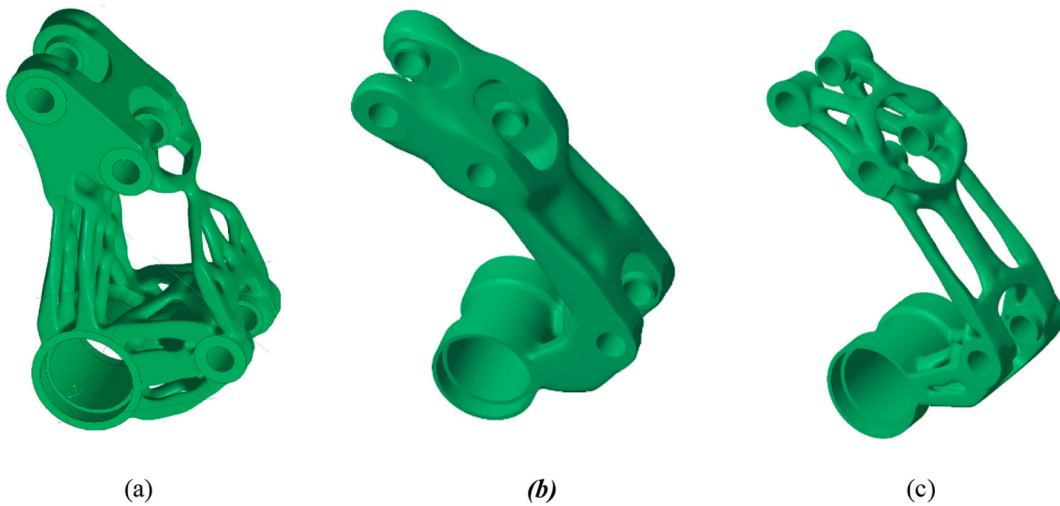

Fig. 11. The output of different generative designs in case of design space version A (a) setup 1, (b) setup 2, (c) setup 3.
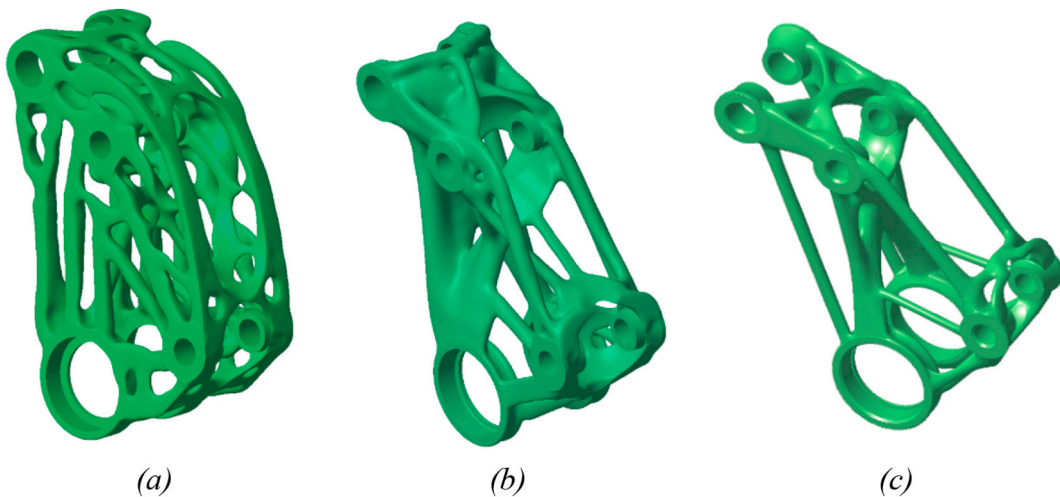

Fig. 12. Output of different generative designs in case of design space version B (a) setup 4, (b) setup 5, (c) setup 6.

which usually causes deformation in the model. For this component, the stress remaining in the model was 200 to 600 MPa.

3.3. Result of validation of printed parts

The validation measurements related to geometry and static and dynamic strength allow the components' approval.

3.3.1. Geometrical validation

Geometric tests revealed that the part warped a few tenths of mm during printing and detachment, but this was not to the extent that it would not have met the requirements. A comparison of the original CAD
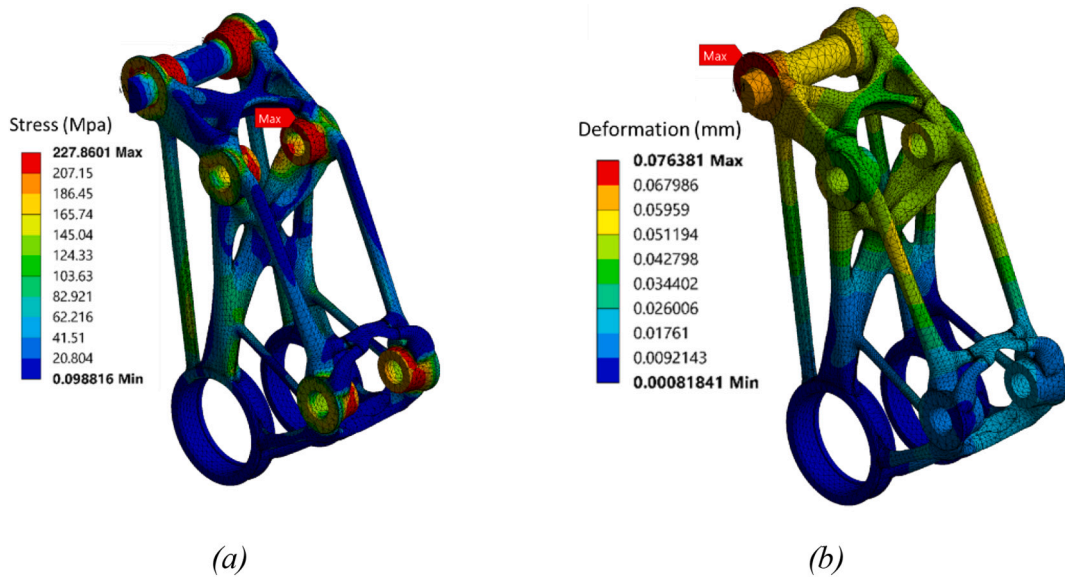
Fig. 13. The result of FEM analysis (a) simulated stresses (b) simulated deformations.

Fig. 14. The printed model fixed on the building platform (a) with inner supports, (b) without inner supports.

Fig. 15. The printed model and the removed support after detaching form the building platform.

model and the CAD model obtained during the geometry measurement of the printed part showed that there was the largest deviation from the original volume outward at a given point, in the middle of the rod, as illustrated in Fig. 19. The maximal geometrical deviation was 0.76 mm.

Since the connecting surfaces of the part are not just printed but post-processed, the deviation does not cause a problem. Therefore, differences in external surfaces, as they are not related to other components, were acceptable. Reducing the unexpected deformations, it is recommended to perform stress-relieving heat treatment when the model and support are on the printing platform. At the current research stage, we
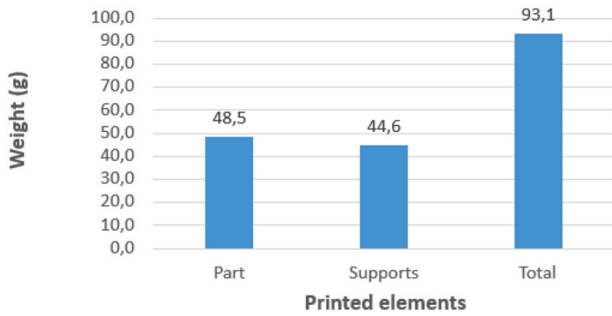
Fig. 16. The weights of the different printed elements.

did not have a way to perform the heat treatments, but it may be recommended to use it later.

3.3.2. Strength validation

The static strength tests revealed that there was still spare material in the part because it was only destroyed under a load of 38,000 N compared with the maximum force (4500 N) used in the simulation and calculated with a safety factor.

The measured forces and elongations carried out in each rod are shown in Fig. 20. Here we can observe what deformation develops in different rods under different loads. In general, the maximal deformation was 0.108 mm for the entire component in the load range used for the test, which was appropriate for us. It can also be seen from the diagrams that the different parts of the component had different stiffness due to the generative design. The most important was rod A1 because this is the most stressed part of the structure. The rigidity marked A4 was the lowest, but it also met our expectations.

3.3.3. Dynamic validation in proving ground

During the tests performed on the ZalaZone proving ground, the data was collected by the motion sensors mounted on the suspension system by FRT colleagues. Based on this data, the loads could be determined indirectly by calculations. The dynamic tests revealed that the load on the part did not exceed the simulated load in any racing situations. After performing the dynamic tests, the printed parts were inspected, and no defects or damage were observed. There was no difference in the driving experience, which can be determined subjectively, so overall, based on the evaluation of the dynamic tests, the application of the new component in the racing car can be approved. Therefore, the part was finally approved.

In Fig. 21 the photos show the built-in rocker during the tests, and the previous and new designs can be seen side by side.

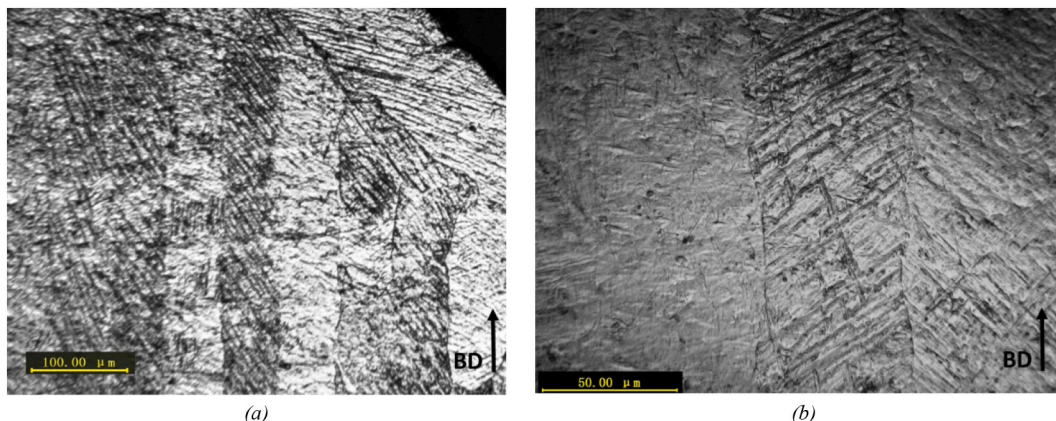Finally, the differences between the original and the new design are

summarized in tabular form. The result shows that with a weight loss of 40 %, the new part has a much higher load capacity and the degree of deformation is a third as high as in the previous case. The related data are shown in Table 5.

4. Conclusions

Summarizing the presented research results, the following points can be summarized:

- A methodology has been developed to ensure better compliance with Formula Student racing car components using generative design and
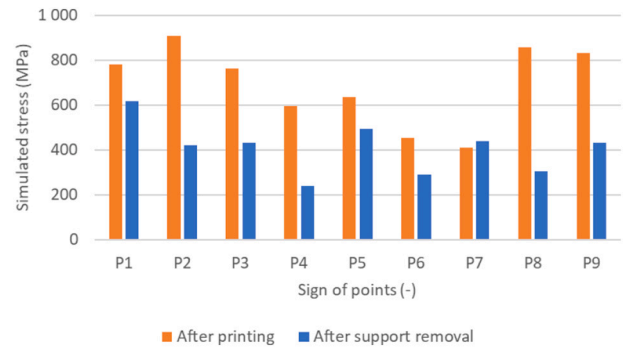

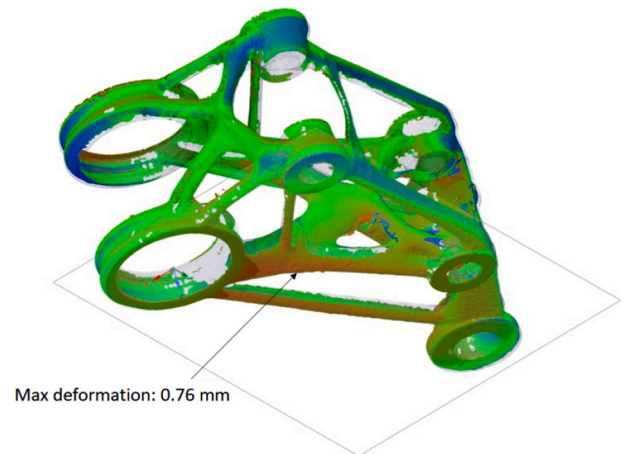**Fig. 18.** The simulated stresses in the model depending on the operation steps.

Fig. 19. The deviation of the CAD and the printed model.

Fig. 17. The micrographs of the printed part (a) columnar prior-β grain structure, (b) the α′ martensite formed inside the prior-β grains (BD: build direction).
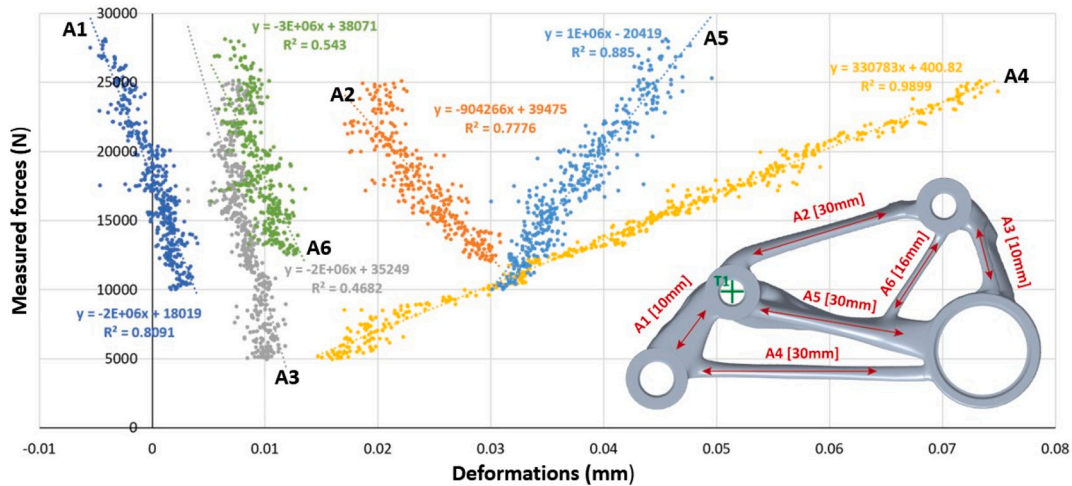
Fig. 20. The measured forces and deformations during the static strength test.
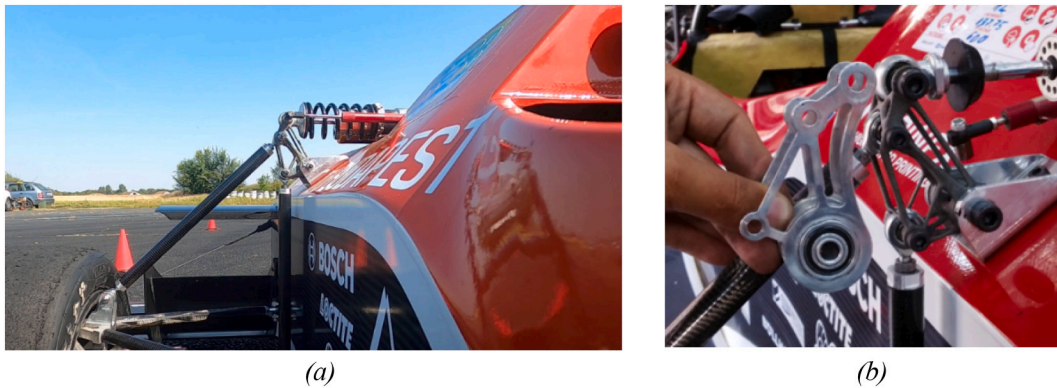

Fig. 21. The built-in rocker part (a) during the test, (b) the original and new design.

Table 5
Comparison of original and new part designs.

Part design	Material	Number of elements (pieces)	Weight (g)	Max. applicable force (N)	Max. deformation at 4500 N (mm)	Max. stress (MPa)
Original	AA 7075	9	85.5	4500	0.270	346
New	Ti6Al4V	1	48.5	38,000	0.108	256

3D metal printing. The developed methodology can be further applied to other components to increase competitiveness.

• Generative design can produce very different results depending on the chosen parameters. Therefore, the interaction of parameters and their effect on geometry and their correct setting is particularly important to generate the appropriate result.

• The control of internal stresses and strains obtained during generative design requires a more professional finite element analysis at the end of the design process.

• Because the titanium base material can be printed with high internal stresses, it is recommended to perform stress-relieving heat treatment after printing because this makes it possible to reduce deformations.

• The rockers in the car's suspension system have been developed with 40 % weight reduction per component and with three times more rigidity and load capacity using less developing time and fewer parts.

• Determining the amount of material used, the weight of the support and the amount of powder extracted during operation of the equipment may be significant relative to the weight of the part. Together, they determine the amount of raw material used.

• The infrastructure of the ZalaZone proving ground is also well-suited for the tests, and the developed dynamic test method is applicable for testing race cars components.

Declaration of competing interest

Acknowledgements

References

[1] Chauhan Parnika, Sah Katya, Kaushal Rashmi. Design, modeling and simulation of suspension geometry for formula student vehicles. Mate. Today Proc. 2021;43(Part 1):17–27.

[2] Walton Dan, Moztar Hadi. Design and development of an additive manufactured component by topology optimization. Procedia CIRP 2017;60:205–10.

[3] Yia Li, Ehmsen Svenja, Glatt Moritz, Aurich Jan C. A case study on the part optimization using eco-design for additive manufacturing based on energy performance assessment. Procedia CIRP 2021;96:91–6.

[4] Liu Jikai, Gaynor Andrew T, Chen Shikui, Kang Zhan, Suresh Krishnan, Takezawa Akihiro, et al. Current and future trends in topology optimization for additive manufacturing. Struct. Multidiscip. Optim. 2018;57:2457–83.

[5] Plocher János, Panesar Ajit. Review on design and structural optimisation in additive manufacturing: towards next-generation lightweight structures. Mater. Des. 2019;183:108164.

[6] Dhokia Vimal, Essink Wesley P, Flynn Joseph M. A generative multi-agent design methodology for additively manufactured parts inspired by termite nest building. CIRP Ann. Manuf. Technol. 2017;66:153–6.

[7] Ahmed Shayaan, Gupt Manoj Kumar. Investigations on motorbike frame material and comparative analysis using generative design and topology optimization. Mate. Today Proc. 2022;56:1440–6 (article in press).

[8] Zhu Jihong, Zhou Han, Wang Chuang, Zhou Lu, Yuan Shangqin, Zhang Weihong. A review of topology optimization for additive manufacturing: status and challenges. Chin. J. Aeronaut. 2021;34(1):91–110.

[9] Emmelmann C, Sander P, Kranz J, Wycisk E. Laser additive manufacturing and bionics: redefining lightweight design. Phys. Procedia 2011;12:364–8.

[10] Seabra Miguel, Azevedo José, Araújo Aurélio, Reis Luís, Pinto Elodie, Alves Nuno, et al. Selective laser melting (SLM) and topology optimization for lighter aerospace componentes. Struct. Integr. Procedia 2016;1:289–96.

[11] Salta Styliani, Papavasileiou Nikolaos, Pyliotis Konstantinos, Katsaros Miltiadis. Adaptable emergency shelter: a case study in generative design and additive manufacturing in mass customization era. Procedia Manuf. 2020;44:124–31.

[12] Wang Hui, Du Wenfeng, Zhao Yannan, Wang Yingqi, Hao Runqi, Yang Mijia. Joints for treelike column structures based on generative design and additive manufacturing. J. Constr. Steel Res. 2021;184:106794.

[13] Rajput Srijan, Burde Himanshu, Singh Udit Suraj, Kajaria Hridik, Bhagchandani Ranjeet Kumar. Optimization of prosthetic leg using generative design and compliant mechanism. Mate. Today Proc. 2021;46:8708–15.

[14] Djokikj Jelena, Jovanova Jovana. Generative design of a large-scale nonhomogeneous structures. IFAC Pap. On Line 2021;54(1):773–9.

[15] Li Shuaishuai, Xin Yanmei, Ying Yu, Wang Yu. Design for additive manufacturing from a force-flow perspective. Mater. Des. 2021;204:109664.

[16] Junk Stefan, Burkart Lukas. Comparison of CAD systems for generative design for use with additive manufacturing. Procedia CIRP 2021;100:577–82.

[17] Marinov Martin, Amagliani Marco, Barback Tristan, Flower Jean, Barley Stephen, Furuta Suguru, et al. Generative design conversion to editable and watertight boundary representation. Comput. Aided Des. 2019;115:194–205.

[18] Gao Wei, Zhang Yunbo, Ramanujan Devarajan, Ramani Karthik, Chen Yong, Williams Christopher B, et al. The status, challenges, and future of additive manufacturing in engineering. Comput. Aided Des. 2015;69:65–89.

[19] García-Domínguez A, Claver J, Sebastián MA. Study for the selection of design software for 3D printing topological optimization. Procedia Manuf. 2017;13:903–9.

[20] Khan Shahroz. Muhammad Junaid Awa: a generative design technique for exploring shape variations. Adv. Eng. Inform. 2018;38:712–24.

[21] Kumara Yogesh, Siddiquia Rehan Abad, Upadhyaya Yogesh, Prajapati Shivam. Kinematic and structural analysis of independent type suspension system with anti-roll bar for formula student vehicle. Mater. Today Proc. 14 October 2021;56:2672–9.

[22] Behandish Morad, Mirzendehdel Amir M, Nelaturi Saigopal. A classification of topological discrepanciesin additive manufacturing. Comput. Aided Des. 2019;115:206–17.

[23] Verma Saurav, Yang Cheng-Kang, Lin Chao-Hsun, Jeng Jeng Ywam. Additive manufacturing of lattice structures for high strength mechanical interlocking of metal and resin during injection molding. Addit. Manuf. 2022;49(102463).

[24] Reinhart Gunther, Teufelhart Stefan. Load-adapted design of generative manufactured lattice structures. Phys. Procedia 2011;12:385–92.

[25] Harl B, Predan J, Gubeljak N, Kegl M. On configuration-based optimal design of load-carrying lightweight parts. Int. J. Simul. Model 2017;16(2):219–28.

[26] Panesar Ajit, Abdi Meisam, Hickman Duncan, Ashcrof Ian. Strategies for functionally graded lattice structures derived using topology optimisation for Additive Manufacturing. Addit. Manuf. 2018;19:81–94.

[27] Wang Zhiping, Zhang Yicha, Tan Shujie, Ding Liping, Bernar Alain. Support point determination for support structure design in additive manufacturing. Addit. Manuf. 2021;47:102341.

[28] Calignano F. Design optimization of supports for overhanging structures in aluminum and titanium alloys by selective laser melting. Mater. Des. 2014;64:203–13.

[29] Li Zhonghua, Zhang David Zhengwen, Dong Peng, Kucukkoc Ibrahim. A lightweight and support-free design method for selective laser melting. Int. J. Adv. Manuf. Technol. 2017;90:2943–53.

[30] Cooper Kenneth, Steele Phillip, Cheng Bo, Chou Kevin. Contact-free support structures for part overhangs in powder-bed metal additive manufacturing. Inventions 2018;3:2. https://doi.org/10.3390/inventions3010002.

[31] Zhang Yicha, Wang Zhiping, Zhang Yancheng, Gomes Samuel, Bernard Alain. Bio-inspired generative design for support structure generation and optimization in Additive Manufacturing (AM). CIRP Ann. Manuf. Technol. 2020;69:117–20.

[32] DebRoy T, Wei HL, Zuback JS, Mukherjee T, Elmer JW, Milewski JO, et al. Additive manufacturing of metallic components – process, structure and properties. Prog. Mater. Sci. 2018;92:112–224.

[33] Hooreweder Brecht VAN, Kruth Jean-Pierre. Advanced fatigue analysis of metal lattice structures produced by Selective Laser Melting. CIRP Ann. Manuf. Technol. 2017;66(1).

[34] Frkana Martin, Konecnaa Radomila, Nicolettob Gianni, Kunz Ludvik. Microstructure and fatigue performance of SLM-fabricated Ti6Al4V alloy after different stress-relief heat treatments. Transp. Res. Procedia 2019;40:24–9.

[35] Mesicek Jakub, Marekpagac, Petru Jana, Novak Petr, Hajnys Jiri, Kutiova Kristyna. Topological optimization of the formula student bell crank. MM Sci. J. October 2019:2964–8.

[36] Sun Li, Deng Zhao, Zhang Qing. Design and strength analysis of FSAE suspension. Open Mech. Eng. J. 2014;8:414–8 (SendOrdersforReprintsto reprints@ benthamscience.ae).

[37] Kaushal Rashmi, Chauhan Parnika, Sah Katya, Chawla VK. Design and analysis of wheel assembly and anti-roll bar for formula SAE vehicle. Mate. Today Proc. 2021;43(Part 1):169–74.

[38] Bikas Harry, Stavridis John, Stavropoulos Panagiotis, Chryssolouris George. A design framework to replace conventional manufacturing processes with additive manufacturing for structural components: a formula student case study. Procedia CIRP 2016;57:710–5.

[39] Walton Dan, Moztarzadeh Hadi. Design and development of an additive manufactured component by topology optimisation. Procedia CIRP 2017;60:205–10.

[40] Samant Saurabh Y, Kumar Santosh, Jain Kaushal Kamal, Behera Sudhanshu Kumar, Gandhi Dhiraj, Raghavendra Sivapuram, et al. Design of suspension system for Formula Student race car. Procedia Eng. 2016;144:1138–49.

[41] Wang Zhiping, Zhang Yicha, Bernard Alain. A constructive solid geometry-based generative design method for additive manufacturing. Addit. Manuf. 2021;41:101952.

[42] Briard Tristan, Segonds Frédéric, Zamariola Nicolo. G-DfAM: a methodological proposal of generative design for additive manufacturing in the automotive industry. Int. J. Interact. Des. Manuf. 2020;14:875–86.

[43] Chuang Ching-Hung, Chen Shikui, Yang Ren-Jye, Vogiatzis Panagiotis. Topology optimization with additive manufacturing consideration for vehicle load path development. Int. J. Numer. Meth. Eng. 2018;113:1434–45.

[44] Xu W, Brandt M, Sun S, Elambasseril J, Liu Q, Latham K, et al. Additive manufacturing of strong and ductile Ti–6Al–4V by selective laser melting via in situ martensite decomposition. Acta Mater. 2015;85:74–84.